NMR IN BIOMEDICINE, VOL. 8, 333–344 (1995)

Inferring Microstructural Features and the Physiological State of Tissues from Diffusion-Weighted Images

Peter J. Basser*

Biomedical Engineering and Instrumentation Program, NCRR, National Institutes of Health, Building 13, Room 3N-17, 13 South Drive, Bethesda, MD 20892-5766, USA

We review several methods that have been developed to infer microstructural and physiological information about isotropic and anisotropic tissues from diffusion weighted images (DWIs). These include Diffusion Imaging (DI), Diffusion Tensor Imaging (DTI), isotropically weighted imaging, and *q*-space imaging. Just as DI provides useful information about molecular displacements in one dimension with which to characterize diffusion in isotropic tissues, DTI provides information about molecular displacements in three dimensions needed to characterize diffusion is anisotropic tissues. DTI also furnishes scalar parameters that behave like quantitative histological or physiological 'stains' for different features of diffusion. These include Trace(D), which is related to the mean diffusivity, and a family of parameters derived from the diffusion tensor, D, which characterize different features of anisotropic diffusion. Simple thought experiments and geometrical constructs, such as the diffusion ellipsoid, can be used to understand water diffusion in isotropic and anisotropic media, and the NMR experiments used to characterize it.

INTRODUCTION

Diffusion imaging (DI), which was first realized in 1985,[1–3] represents a landmark contribution in the history of NMR. Diffusion imaging consists of estimating an effective scalar diffusivity[4] from a set of diffusion weighted images (DWIs). As such, DI is one of only a handful of MRI modalities that provides a measurement or map of a fundamental physical quantity. The myriad of applications and the underlying principles of diffusion imaging are well known to many MR practitioners, and are the subjects of a number of excellent books and review articles.[4,5]

In this review we examine several new approaches to inferring microstructural and/or physiological information about tissues from diffusion weighted images. We will focus particularly on new methods to characterize diffusion in anisotropic tissues such as brain white matter, kidney, and skeletal and cardiac muscle, in which the apparent diffusion coefficient (*ADC*) has been observed to vary with the tissue's orientation.[6–13] In these tissues diffusion imaging, which measures one-dimensional molecular displacements, inherently does not provide enough information to characterize the three-dimensional translational displacements of protons (or other labeled nuclei). We will also describe different models relating molecular displacement and the measured NMR signal in tissues and their uses (and abuses) in interpreting diffusion weighted images and spectra (particularly their use in characterizing the degree of isotropic or anisotropic diffusion in tissues). Moreover, we will examine several new approaches to inferring information about tissue orientation from DWIs and diffusion spectra. We will not, however, describe the gradient hardware, the sequences used to acquire DWIs and other technical matters that do not pertain directly to the theory of measuring diffusive transport coefficients using NMR or the post-processing of DWIs, as they are the subject of other reviews in this journal, as well as of recent review articles.[5]

Since the review is an outgrowth of a lecture given at the recent London workshop on Diffusion Imaging,[14] it has a tutorial character. Instead of using formal arguments, which rely heavily on evaluating complicated integrals and manipulating tensors, we will present our arguments about diffusion more intuitively, using throughout experiments, diagrams, statistical reasoning and a little analytical geometry. One geometric construct that is proving to be particularly useful for characterizing diffusion in both isotropic and anisotropic media is the "diffusion ellipsoid".[15,16] Another new and useful geometric construct in understanding the measurement of the three-dimensional effective displacement distribution using MR techniques is the "measurement ellipsoid". A great deal of information needed to characterize and measure effective diffusion in tissues is contained in their size, orientation, shape and their distribution within the tissue.

BACKGROUND

Diffusion imaging (DI) provides an estimate of a single scalar apparent diffusion constant (*ADC*) in each voxel from a series of diffusion weighted images (DWIs) using linear regression of eq. (1) below:

$$\ln\left(\frac{A(b)}{A(0)}\right) = -bD = -b\,ADC, \qquad (1)$$

where: $A(b)$ is the measured echo signal in each voxel; b is a constant that Le Bihan called the b-value or b-factor, which is calculated for each gradient pulse sequence;[17] $A(0)$ is the signal intensity for $b=0$. Whether one is acquiring DWIs or *ADC* maps, diffusion imaging using eq. (1) is inherently a one-dimensional technique. By that we mean that it can incorporate information about molecular displacements in one direction only even if the particle motion

* Author to whom correspondence should be addressed.

CCC 0952–3480/95/070333–12

Received 20 September 1995
Accepted (revised) 8 December 1995

itself is three-dimensional.

Diffusion tensor imaging (DTI)[15] is a new MRI modality that was developed to describe diffusion in an anisotropic medium for which eq. (1) is no longer adequate. With DTI, one estimates an effective diffusion tensor, **D**, from DWIs using a more general relationship between the measured echo magnitude in each voxel and all the imaging and diffusion gradient sequences:[18–20]

$$\ln\left(\frac{A(b)}{A(0)}\right) = -\sum_{i=1}^{3}\sum_{j=1}^{3} b_{ij}D_{ij} = -(b_{xx}D_{xx} + 2b_{xy}D_{xy} + 2b_{xz}D_{xz} + b_{yy}D_{yy} + 2b_{yz}D_{yz} + b_{zz}D_{zz}). \quad (2)$$

Above, b_{ij} is a component of the symmetric b-matrix, **b**. Whereas the b-factor in DI is calculated for a gradient sequence applied only in one direction, the b-matrix in DTI is calculated from all three applied gradient sequences (including all imaging and diffusion gradient sequences).[18–20]* Above, we write the echo intensity for a gradient sequence whose b-matrix is **b** as $A(\mathbf{b})$. It only recently became possible to measure each component of **D**, D_{ij} from DWIs. This was done by performing multivariate linear regression of eq. (2) using a series of DWIs in which diffusion gradients with different amplitudes were applied in a multiplicity of directions.[18, 20] Figure 1 depicts the steps one performs to obtain (a) a "diffusion image" or "map" and (b) a "diffusion tensor image" from a set of diffusion weighted images.

Diffusion tensor imaging subsumes diffusion imaging. Note that for an isotropic sample eq. (2) reduces to the form of eq. (1):

$$\ln\left(\frac{A(b)}{A(0)}\right) = -(b_{xx} + b_{yy} + b_{zz})D. \quad (3)$$

If we set the b-factor in eq. (1) equal to the coefficient of the diffusivity in eq. (3), i.e.

$$b = b_{xx} + b_{yy} + b_{zz}, \quad (4)$$

then these two models are equivalent. Interestingly, even for diffusion imaging of isotropic media, not all the contributions produced by imaging and diffusion gradients are presently being taken into account.

* In diffusion imaging, the single scalar b-factor we calculate for each DWI contains interactions among (a) diffusion gradient pulses, (b) diffusion and imaging gradient pulses, and (c) imaging gradient pulses, which are all applied along the same direction.[4] In diffusion tensor imaging, the b-matrix we calculate for each DWI contains the interactions among (a) diffusion gradient pulses, (b) diffusion and imaging gradient pulses, and (c) imaging gradient pulses, which may be applied along the same direction or along perpendicular directions.[18–20] Just as in diffusion imaging, in diffusion tensor imaging the contributions of imaging gradients on the phase distribution of the spin system may be significant, i.e. they may affect the magnitude of the measured echo in each voxel, and thus our estimate of the diffusion tensor.[18] Clearly in DTI, accounting for the coupling between these various gradient pulses in parallel and perpendicular directions and assessing their effect on the measured echo is more complicated than in DI. To facilitate this process, analytic expressions for the b-matrix have been derived for various commonly used MRI sequences.[18, 20, 21]

PRIMER ON ISOTROPIC AND ANISOTROPIC DIFFUSION

First, it is useful to provide a brief introduction to the notions of isotropic and anisotropic diffusion, and to

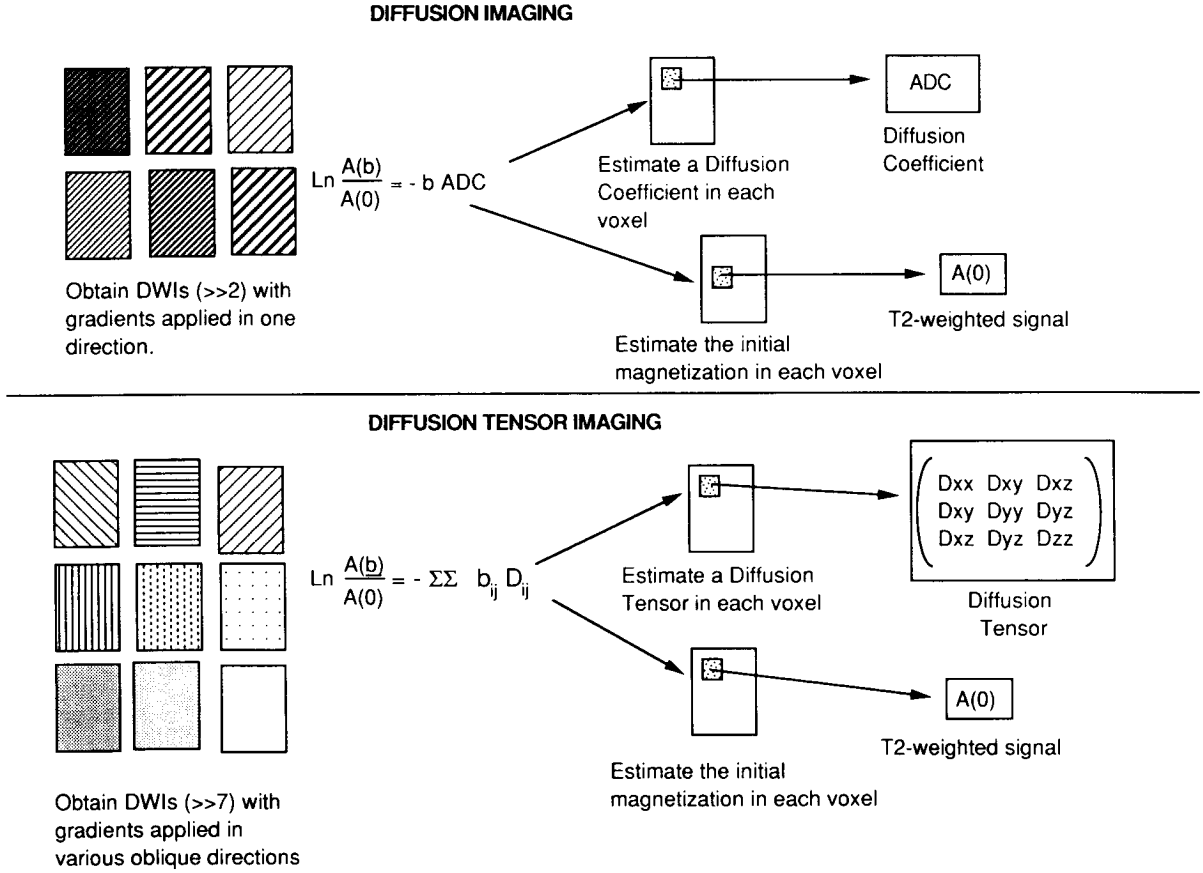

Figure 1. Chart comparing the steps involved in performing diffusion imaging (DI) and diffusion tensor imaging (DTI). Just as DI produces a diffusion coefficient and a T_2-weighted scalar, $A(0)$ in each voxel, DTI produces a 3×3 diffusion tensor and a T_2-weighted scalar, $A(0)$ in each voxel.

characterizing translational diffusion in isotropic and anisotropic media. Diffusion anisotropy is a property of certain media in which the translational mobility of the diffusing molecule depends upon the medium's orientation. Diffusion isotropy describes the condition in which the translational mobility of the diffusing molecule is independent of the medium's orientation.

Diffusion of a water droplet in a jar of water—isotropic diffusion

Suppose we placed a droplet of water in the center of a tank filled with water. We imagine that the water molecules in the drop could be visualized as though they were colored. Some time after release, the water molecules will redistribute themselves within the container owing to the random collisions between them. Their displacement profile[22] is given by:

$$\rho(\mathbf{r}|\tau_d)=\frac{1}{\sqrt{(4\pi D\tau_d)^3}}\exp\left(\frac{\mathbf{r}^T\mathbf{r}}{4D\tau_d}\right)=\frac{1}{\sqrt{(4\pi D\tau_d)^3}}\times\exp\left(-\frac{x^2+y^2+z^2}{4D\tau_d}\right). \quad (5)$$

Above, $\rho(\mathbf{r}|\tau_d)$ is the probability that a particle initially at position $\mathbf{r}=0$, is at position $\mathbf{r}$ at a later time τ_d. These surfaces are concentric spheres ("diffusion spheres") which we obtain by setting the exponent of eq. (5) to a constant. An example is given in Fig. 2. One particularly convenient choice is $-\frac{1}{2}$. Then,

$$x^2+y^2+z^2=(\sqrt{2D\tau_d})^2. \quad (6)$$

In this case, the radius of the diffusion sphere is $\sqrt{2D\tau_d}$, which is also the standard deviation, σ, of $\rho(\mathbf{r}|\tau_d)$. By the well-known Einstein formula:[22]

$$\sigma=\sqrt{2D\tau_d}, \quad (7)$$

the radius of the diffusion sphere is the mean-squared displacement of a particle from the center of the sphere in time τ_d. We also see that the translational displacement profile of water is completely specified by a single scalar constant, D, the diffusion coefficient, and the diffusion time, τ_d.

Diffusion of water in a homogeneous, anisotropic medium

Suppose that we again placed a drop of water in a homogeneous, anisotropic medium. The displacement distribution is now slightly more complicated:

$$\rho(\mathbf{r}|\tau_d)=\frac{1}{\sqrt{|D|(4\pi\tau_d)^3}}\exp\left(\frac{-\mathbf{r}^T\mathbf{D}^{-1}\mathbf{r}}{4\tau_d}\right). \quad (8)$$

Whereas for an isotropic medium D appeared in the variance of the distribution [Eq. (5)], for an anisotropic medium $\mathbf{D}$ appears as the "matrix of variances and covariances"[23] [Eq. (8)]. Where D^3 appeared in the normalization factor of the probability density function, now $|\mathbf{D}|$ (the determinant of $\mathbf{D}$) appears in its place. When we construct surfaces of constant probability (again by setting the exponent of the displacement distribution to a constant), we obtain instead:

$$(D_{yy}D_{zz}-D_{yz}^2)x^2+2(D_{xz}D_{yz}+D_{xy}D_{zz})xy+(D_{xx}D_{zz}-D_{xz}^2)y^2+2(D_{xy}D_{yz}-D_{xz}D_{yy})xz+2(D_{xy}D_{xz}-D_{xx}D_{yz})yz+(D_{xx}D_{yy}-D_{xy}^2)z^2=|\mathbf{D}|\tau_d, \quad (9a)$$

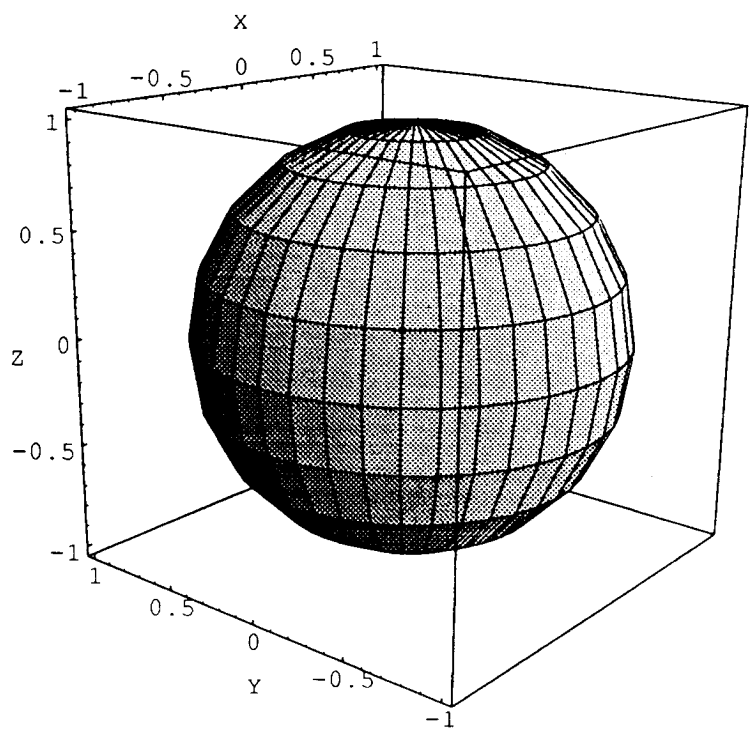

Figure 2. Diffusion sphere indicating the hypothetical surface of constant mean-squared displacement one would expect in an isotropic medium.

which, when rewritten in "canonical form":

$$ax^2+2b\,xy+dy^2+2c\,xz+2e\,yz+fz^2$$

$$=(x\,y\,z)\begin{pmatrix} a & b & c \\ b & d & e \\ c & e & f \end{pmatrix}\begin{pmatrix} x \\ y \\ z \end{pmatrix}=1, \qquad (9b)$$

is seen to be the equation of a (three-dimensional) ellipsoid†, which is called the "diffusion ellipsoid".[15,16] An example of a diffusion ellipsoid is shown in Fig. 3.

Clearly, in an anisotropic medium, more information is required to describe the three-dimensional displacement of particles than in an isotropic medium. Equivalently, in anisotropic media more information is required to specify the size, shape and orientation of the diffusion ellipsoid than in isotropic media. Where one parameter, D, was sufficient for an isotropic medium, now six independent parameters (a–f, above, or the six coefficients of $\mathbf{D}$, D_{xx}, D_{yy}, D_{zz}, D_{xy}, D_{xz}, and D_{yz}) are required for an anisotropic one. This is so because in anisotropic media, displacements generally appear to be correlated in the x, y and z directions, whereas in isotropic media they do not. Physically, this is because the structure of the anisotropic medium biases the translational motions of molecules along particular directions and away from others. The elements of the diffusion tensor represent correlations between these molecular translational displacements. Its diagonal elements, D_{xx}, D_{yy} and D_{zz}, represent correlations along the same directions, x, y and z, respectively, while its off-diagonal elements, D_{xy}, D_{xz} and D_{yz}, represent correlations between molecular translational displacements in perpendicular or orthogonal directions, i.e. between x and y, x and z and y and z, respectively. In isotropic media the diagonal elements of the diffusion tensor are all equal, whereas in anisotropic media they usually are not. Moreover, in isotropic media the off-diagonal elements are always zero, but in anisotropic media they may be large (i.e. comparable in magnitude to the diagonal elements).

We can always find a frame of reference, usually one other than the laboratory frame, in which these translational displacements appear to be uncorrelated. This is called the "principal frame". Its axes are coincident with the principal axes of the diffusion ellipsoid. In this frame all off-diagonal elements of $\mathbf{D}$ vanish, and the equation describing the diffusion ellipsoid, eq. (9), assumes a simpler and more familiar form:

$$\left(\frac{x'}{\sqrt{2\lambda_{xx'}\tau_d}}\right)^2+\left(\frac{y'}{\sqrt{2\lambda_{yy'}\tau_d}}\right)^2+\left(\frac{z'}{\sqrt{2\lambda'_{zz}\tau_d}}\right)^2=1. \qquad (10)$$

Above, λ'_{xx}, λ'_{yy} and λ'_{zz} are the principal diffusivities in the x', y' and z' coordinated system that is coincident with the principal directions; $\sqrt{2\lambda'_{xx}\tau_d}$, $\sqrt{2\lambda'_{yy}\tau_d}$ and $\sqrt{2\lambda'_{zz}\tau_d}$ represent the mean-squared displacements of a molecule in the (three principal) x', y' and z' directions at time τ_d, respectively. These quantities are also the major and minor axes of the diffusion ellipsoid. It is worth noting that in MRI applications, the principal axes of the diffusion ellipsoid are generally not coincident with the x-y-z laboratory axes, nor are these principal directions and diffusivities known *a priori*.

From these intuitive and simple geometric arguments, we can already see that both the diagonal and off-diagonal elements of $\mathbf{D}$ are essential in determining the size, shape and orientation of the diffusion ellipsoid, and thus characterizing diffusion in anisotropic media. Algebraically, this can be demonstrated by referring to eq. (9a) or by writing other quantities that characterize the ellipsoid's features (such as the distance between its foci and center, or the eccentricity of the three great ellipses) in terms of these quantities. It is also easy to see by referring to Fig. 4 that diagonal elements of the diffusion tensor, D_{xx}, D_{yy} and D_{zz},

† This is true because $\mathbf{D}$ and the coefficient matrix are both positive definite.

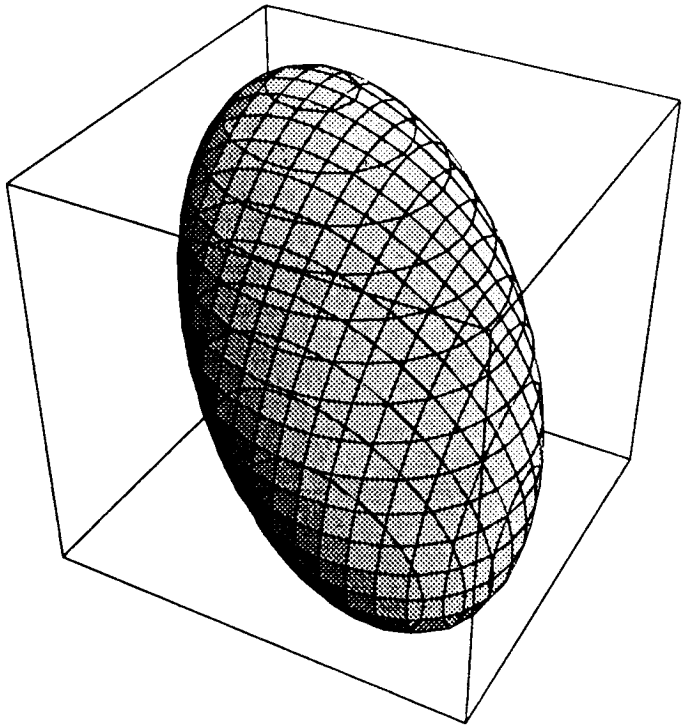

Figure 3. Diffusion ellipsoid showing the hypothetical surface of constant mean-squared displacement one would expect in an anisotropic medium.

are alone not sufficient to characterize the size, shape and orientation of the diffusion ellipsoid.

THE MEASUREMENT OF THE DIFFUSION COEFFICIENT AND THE DIFFUSION TENSOR—A GEOMETRIC VIEW

We can interpret the measurement of the diffusion tensor geometrically from the relationship between the measured echo and the diffusion tensor, eq. (2). In diffusion tensor spectroscopy, in which there are only diffusion gradients applied in a particular direction, but no imaging (localization) gradients, we can write this relationship as:

$$\ln\left(\frac{A(\mathbf{G})}{A(0)}\right) = -\alpha^2|\mathbf{G}|^2\,\hat{\mathbf{r}}^{\mathrm{T}}\,\mathbf{D}\,\hat{\mathbf{r}} \qquad (11)$$

where the applied gradient $\mathbf{G}$ is written as $|\mathbf{G}|\,\hat{\mathbf{r}}$, where $\hat{\mathbf{r}}$ is a unit vector in the direction of the applied diffusion gradient, and α^2 is a parameter that is calculated from the pulse sequence.[20] Above, the symbol "T" indicates the transpose operation. It is helpful to consider an experiment in which the diffusion gradient strengths and directions are chosen so that the measured echo intensity is constant, independent of gradient direction. For an isotropic medium (i.e. $\mathbf{D}=D\,\mathbf{I}$, where $\mathbf{I}$ is the identity or unit tensor), eq. (11) reduces to

$$\text{constant} = -\ln\left(\frac{A(\mathbf{G})}{A(0)}\right) = \alpha^2|\mathbf{G}|^2 D\,\hat{\mathbf{r}}^{\mathrm{T}}\,\mathbf{I}\,\hat{\mathbf{r}} = \alpha^2|\mathbf{G}|^2 D, \qquad (12)$$

which is the equation of a sphere in a space whose coordinate axes are $\sqrt{b_{xx}}$, $\sqrt{b_{yy}}$ and $\sqrt{b_{zz}}$. Regardless of the direction of the applied diffusion sensitizing gradient, we obtain the same diffusivity, D. Therefore, we view the measurement of the diffusivity in an isotropic medium as specifying a point on this measurement sphere. In practice, owing to experimental noise, we cannot measure the diffusivity with one experiment. Moreover, since $A(0)$ is an unknown, we also need to determine it. Therefore, in principle, we could measure the mean diameter of a cluster of points on the measurement sphere. This could be done for example, by sampling many different points on the measurement sphere and then finding the radius that minimizes the sum of the distances between the data points and points on the surface of the sphere. However, usually it is done by applying diffusion gradients in only one direction and varying the gradient strength for a fixed diffusion time.

By analogy, in anisotropic media, estimating the diffusion tensor is tantamount to determining the measurement surface given in eq. (11), which we immediately recognize as another ellipsoid, since it can be recast in the same form as eq. (9b):

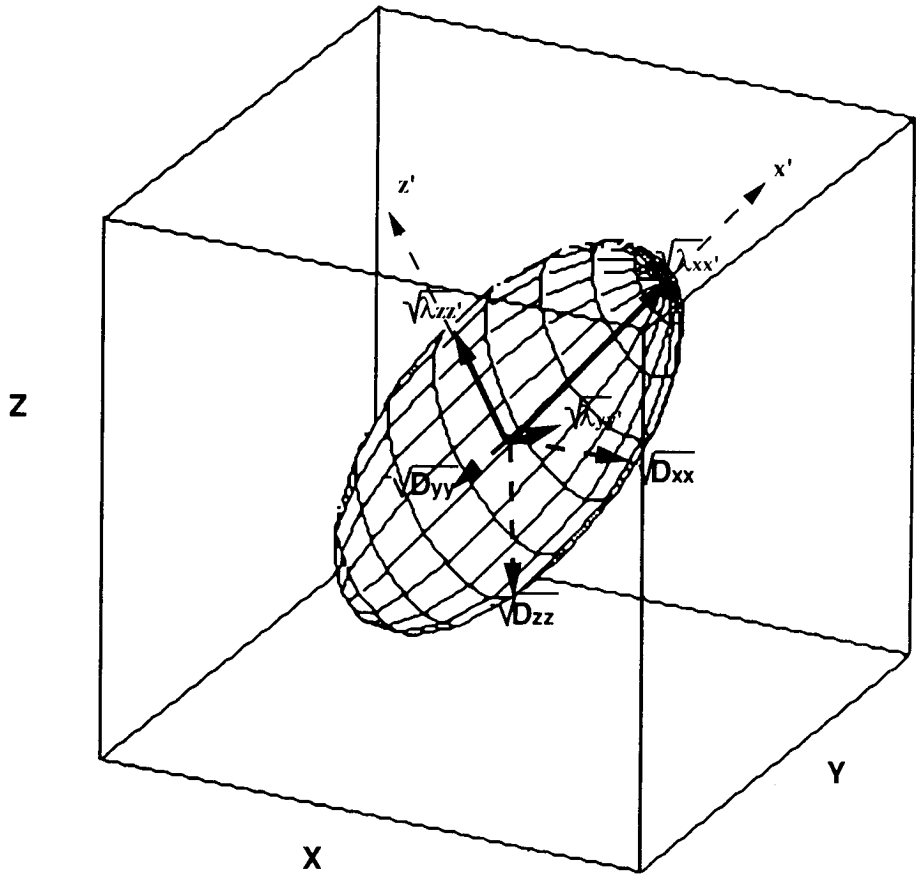

Figure 4. A diffusion ellipsoid. The major and minor axes are proportional to the square roots of the eigenvalues of the diffusion tensor; the square roots of the diagonal elements of the diffusion tensor, D_{xx}, D_{yy} and D_{zz} are also depicted as the line segments between the center and the surface of the ellipsoid which lie on the *x*-, *y*- and z-axes, respectively. We see that the diagonal elements of **D** alone are not sufficient to characterize the size, shape and orientation of the diffusion ellipsoid—all elements of the diffusion tensor are required. For ease of illustration, the diffusion time, τ, is taken to be $\frac{1}{2}$.

$$a'x^2+2b'xy+d'y^2+2c'xz+2e'yz+f'z^2 = (x\ y\ z)\begin{pmatrix} a' & b' & c' \\ b' & d' & e' \\ c' & e' & f' \end{pmatrix}\begin{pmatrix} x \\ y \\ z \end{pmatrix} = 1. \quad (13)$$

The measurement ellipsoid also requires six independent parameters to specify its size, shape and orientation, which, like the diffusion ellipsoid, can also be calculated from the six independent components of the diffusion tensor. However, the measurement and diffusion ellipsoids do not have the same size, shape and orientation. Although their principal directions or principal axes coincide, their corresponding major and minor axes are reciprocals of one another. Figure 5 shows the measurement ellipsoid that corresponds to the diffusion ellipsoid shown in Fig. 3. Therefore, where the measurement ellipsoid is elongated, the diffusion ellipsoid is shortened and *vice versa*. These two "reciprocal" surfaces illustrate the fact that the effective displacement distribution of molecules (**x**-space representation) is the Fourier transform of the net magnetization distribution.[24]

Finally, the measurement ellipsoid construction helps us visualize how the ADC measured in a particular direction is related to the diffusion tensor. The term $\hat{\mathbf{r}}^T\ \mathbf{D}\ \hat{\mathbf{r}}$ in eq. (11) represents the projection of the diffusion tensor along the diffusion sensitizing gradient direction $\hat{\mathbf{r}}$, and thus is the "*ADC*" we measure in a spectroscopic experiment (i.e. without localizing gradients) with diffusion sensitizing gradients pointing in the $\hat{\mathbf{r}}$ direction. While the diagonal elements of the diffusion tensor D_{xx}, D_{yy} and D_{zz} represent *ADC*s along the x, y and z directions, respectively, the off-diagonal elements, D_{xy}, D_{xz} and D_{yz}, do not represent *ADC*s

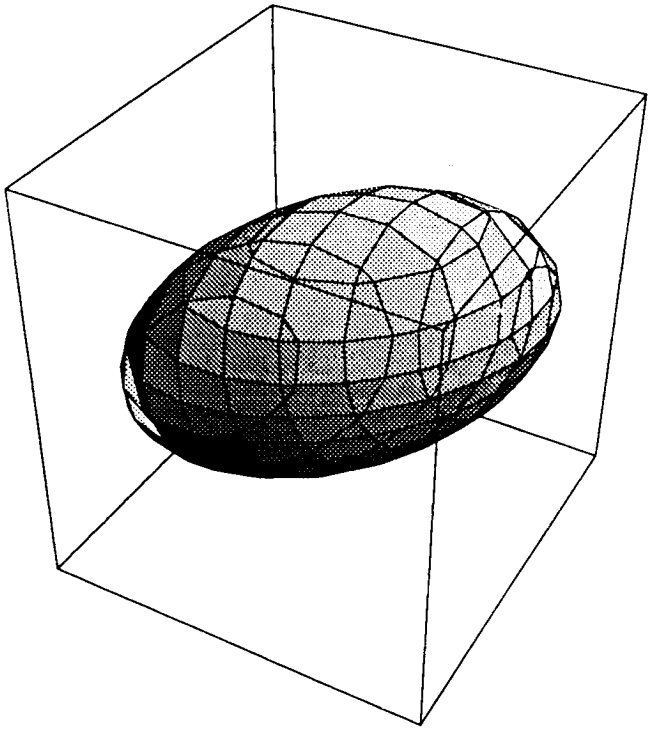

Figure 5. The measurement ellipsoid that corresponds to the diffusion ellipsoid in Fig. 3. The measurement ellipsoid also requires the six independent elements of the diffusion tensor to specify its size, shape and orientation. However, the measurement and diffusion ellipsoids do not have the same size, shape and orientation. Although their principal directions or principal axes coincide, their corresponding major and minor axes are reciprocals of one another.

obtained by applying equal strength gradients simultaneously in x and y, x and z and y and z. For example, with diffusion gradients applied only in the x-direction, eq. (11) becomes

$$\ln\left(\frac{A(\mathbf{G})}{A(0)}\right) = -\alpha^2 G_x^2 D_{xx} = -\alpha^2 G_x^2\, ADC. \quad (14)$$

D_{xx}, the *ADC* in the x-direction, can be identified as being proportional to the point of intersection of the center of the measurement ellipsoid and the x-axis. With equal gradients applied along both the x- and y-directions, $G_x = G_y = G$, eq. (11) becomes

$$\ln\left(\frac{A(\mathbf{G})}{A(0)}\right) = -\alpha^2 G^2 (D_{xx}+2D_{xy}+D_{yy}) = -\alpha^2 G^2\, ADC'. \quad (15)$$

ADC' contains contributions from D_{xx}, D_{yy} and D_{xy} so it is clear that D_{xy} is not the same as *ADC'*.

The measurement ellipsoid construction can be used to explain why even in a noise-free experiment, we must apply diffusion gradients in at least six different (noncollinear) directions in order to estimate all the independent elements of **D**—since that is the smallest number of noncollinear points required to specify the size, shape and orientation of the measurement ellipsoid. However, because of measurement noise, it is necessary to obtain more data, by applying gradients in more than six noncollinear directions or by performing multiple acquisitions along those six directions. This former is particularly important if a material's measurement ellipsoid is very elongated, such as in the corpus callosum of human and monkey white matter.[25] There, the length of the major axis of the diffusion ellipsoid can easily be underestimated unless diffusion gradients are applied nearly parallel to this principal direction.

Finally, the diffusion and measurement ellipsoids help us to represent experimental noise that corrupts the estimates of diffusion coefficients and diffusion tensors. Without noise, we could consider the diffusion and measurement ellipsoids to be well-defined, infinitesimally thin shells. However, in the presence of noise, we must think of them rather as thick-walled, fuzzy ellipsoids (i.e. with a surface roughness). The thickness of this surface fuzz may not be uniform, and is related to the S/N of the DWIs, the material in the voxel and the set of diffusion gradients (both strength and direction) that we apply. Measurement noise will affect our estimate of *ADC*s and diffusion tensors, as well as their eigenvalues (the principal diffusivities) and eigenvectors (the principal directions). Generally, the smaller the S/N, the thicker the fuzz, and the more the measurement surface will deviate from being ellipsoidal.

DIFFUSION TENSOR IMAGING—APPLICATIONS TO CHARACTERIZING ISOTROPY AND ANISOTROPY

Clinical importance of characterizing the isotropic component of diffusion

Characterizing the isotropic part of the diffusion tensor has become increasingly important clinically since Moseley *et al.*[26,27] and Minotorovitch *et al.*[28] discovered in animals, and Chien *et al.*[29] and Warach *et al.*[30] later showed in humans

that a reduction in the *ADC* is a sensitive indicator of the onset and severity of cerebral ischemia. However, from their earliest work, it was clear that while in gray matter compartments (where diffusion is approximately isotropic) the *ADC* was independent of the direction of the diffusion sensitizing gradients, in white matter this was not the case. There, the contrast of the DWI or the calculated value of the *ADC* in a voxel depended upon the direction in which the diffusion sensitizing gradient was applied with respect to the orientation of the white matter fiber tracts. This orientationally dependent contrast complicated the interpretation of these images in anisotropic white matter. Specifically, one could not ascertain whether hyper- or hypo-intensity in a region of white matter resulted from a structural/physiological change (brought on by the ischemic event), or from diffusion anisotropy in the tissue (i.e. the sensitivity of the *ADC* to the orientation and strength of the applied diffusion gradient). In this particular application of diffusion imaging, tissue anisotropy produced an unwanted experimental artifact.

Diffusion tensor spectroscopy[19, 31] and diffusion tensor imaging[15, 32] provided a solution to this vexing problem. Associated with each diffusion tensor are scalar quantities known as scalar invariants that are intrinsic to the medium. Specifically, they are independent of the laboratory frame of reference (in which the components of the diffusion tensor are measured) and the direction or orientation of the structures that reduce the observed diffusion anisotropy. Therefore, these parameters (or functions of them) are independent of the orientation of the structures, the patient within the MR magnet, the direction of the applied imaging and diffusion sensitizing gradients and the choice of the laboratory coordinate system.[15, 33] These scalar invariants were first proposed in 1992 as novel MR imaging parameters[31] that were shown experimentally to be independent of fiber tract direction in diffusion spectroscopic studies in anisotropic skeletal muscle.[31]

The Trace of the diffusion tensor

One of the aforementioned scalar invariants we proposed, Trace(**D**),

$$\text{Trace}(\mathbf{D}) = D_{xx} + D_{yy} + D_{zz} = 3\langle D \rangle = \lambda_{xx'} + \lambda_{yy'} + \lambda_{zz'}, \qquad (16)$$

is proportional to the orientationally averaged (or "isotropically averaged") apparent diffusivity.[34] Geometrically, Trace(**D**) is also proportional to the sum of the squares of the major and minor axes of the diffusion ellipsoid. To see this, note that the mean-squared displacement in the *i*th principal direction, $\langle r_i^2 \rangle$, is given by:

$$\langle r_i^2 \rangle = 2\lambda_i \tau, \qquad (17)$$

in a diffusion time τ. Then the average of the mean-squared displacements along the three principal directions, $\langle\langle r^2 \rangle\rangle$, is

$$\langle\langle r^2 \rangle\rangle = \frac{\langle r_{x'}^2 \rangle + \langle r_{y'}^2 \rangle + \langle r_{z'}^2 \rangle}{3} = 2\,\frac{\lambda_{xx'} + \lambda_{yy'} + \lambda_{zz'}}{3}\,\tau = 2\langle D \rangle \tau. \qquad (18)$$

van Gelderen *et al.*[35] subsequently used the "trace" as an imaging parameter in an *in vivo* study of a model of cerebral ischemia in cats, claiming the superiority of the "trace" to the *ADC* in defining the ischemic region because it removes the orientational dependence inherent in the *ADC*. This group defines the "trace" differently from eq. (16). Their "trace" is obtained by summing *ADC*s measured in three orthogonal directions:[35]

$$\text{"Trace"} = ADCx + ADCy + ADCz = 3\langle ADC \rangle, \qquad (19)$$

where each *ADC* is estimated from the diffusion imaging equation, eq.(1).[36] Moreover, in calculating the *b*-factor in eq. (1), they use only the "Stejskal–Tanner" terms, ignoring the contributions of all imaging gradients on the measured echo. The Stejskal–Tanner formula,[36] although widely used in diffusion imaging, was derived specifically for diffusion spectroscopy, not for diffusion imaging, which had not yet been invented. In contrast, the definition of Trace(**D**) used by Basser *et al.*[15, 31] in diffusion tensor imaging is that given in eq. (16), where **D** is estimated using eq. (2) in which the effects of all the imaging and diffusion gradients on the echo signal are accounted for.

The disagreement between these two methods is not merely of academic interest. Only when there are no localization gradients or when all cross-terms can be shown to vanish will eq. (16) be equivalent to eq. (19) and will be guaranteed to independent of the tissue's orientation. Otherwise, the "trace" defined in eq. (19) will depend on the orientation of anisotropic structures. This is because the "trace" is calculated using an isotropic model of diffusion—eq. (1). In general, without including the effect of all the diagonal and off-diagonal elements of the diffusion tensor on the signal attenuation, the estimate of the diagonal elements of the diffusion tensor will be in error, and so will their sum or mean value. The "trace" is calculated without considering the phase dispersion of the nuclear spins due to the imaging gradients. If the imaging gradients produce significant cross-terms, as they would for example in diffusion weighted MR microscopy sequences, or in imaging sequences in which imaging gradients are not immediately refocused, then significant additional orientational artifacts can be introduced. Nonetheless, if the biological effect of interest can be demonstrated to be significantly larger than any of the errors introduced by using eq. (19), then the "Trace" is still preferable to the *ADC* in anisotropic media when one wants to mitigate the effect of fiber orientation.

The significance of these potential artifacts can be assessed quantitatively by performing a simple experiment. One can obtain a set of DWIs with diffusion sensitizing in any three orthogonal directions, and then repeat the acquisition with diffusion sensitizing gradients applied in three new (skewed) mutually orthogonal directions. This data set is then used to obtain two independent estimates of the "trace" or the mean *ADC*. The aggregate data set can also be used to estimate a single diffusion tensor, **D**, from which Trace(**D**), given in eq. (16), can be calculated. One can then compare the two estimates of the "trace" to each other, as well as to Trace(**D**).

It would be disingenuous to suggest that eq. (2) is no more time consuming or resource intensive to implement than eq. (1), and that three *ADC*s are not simpler to estimate than the six elements of a diffusion tensor. Nevertheless, if the material is anisotropic, eq. (1) is not an adequate model of diffusion. However, the development of fast high-resolution DW imaging[37, 38] as well as user-friendly software with which diffusion tensors can be readily estimated, and images derived from them displayed, has significantly mitigated this problem, making the trade-off in effort and time between diffusion imaging and diffusion tensor imaging much less severe. If one is only interested in

measuring Trace(**D**), a reasonable alternative may be to obtain isotropically weighted sequences.

Isotropically weighted sequences

In a clinical setting, for example, in the evaluation of stroke patients, total scan time is critical. One of the principal disadvantages of calculating Trace(**D**) from the estimated diffusion tensor (or even calculating the "trace") is that obtaining enough high quality, motion-artifact free, high-resolution DWIs may still be too time consuming. Moreover, these DWIs must be post-processed to produce the final map or image. In acute cases, a need exists to identify DWI sequences that require no significant post-processing, but whose contrast [like Trace(**D**)] is independent of the orientation of structures within the brain or other tissues.

An interesting first step in this area was taken by Edelman *et al.*[39] who attempted to remove the orientational artifact by taking the sum of diffusion weighted images with gradients applied in the x, y and z directions:

$$\mathrm{DWI}_{xx}+\mathrm{DWI}_{yy}+\mathrm{DWI}_{zz}=3\langle\mathrm{DWI}\rangle. \tag{20}$$

The average DWI, $\langle\mathrm{DWI}\rangle$, is intended to remove the orientational artifact caused by anisotropic diffusion [like Trace(**D**)]. Even if the imaging gradients can be chosen to have a negligible effect on the measured signal attenuation, the quantity above is usually not a reasonable proxy for Trace(**D**)/3 owing to its strong T_1 and T_2 weighting. A more quantitative approach has been to develop single-shot "isotropically weighted" DWI sequences whose image contrast is proportional to Trace(**D**). Two such sequences were recently proposed.[40–42] Mori and van Zijl[41] obtained isotropically weighted images by applying a tetrahedral pattern of bi-polar diffusion gradients, producing a DWI in which the signal attenuation would be independent of the off-diagonal elements of the diffusion tensor and would be equally sensitive to the attenuation produced by each of the diagonal elements, D_{xx}, D_{yy} and D_{zz}. The contribution of the imaging gradients to the signal attenuation is mitigated by immediately refocusing each diffusion gradient pulse. This clever strategy to eliminate "cross terms", however, greatly reduces the sequence's diffusion weighting or attenuation. This is because when the bi-polar diffusion gradients are adjacent to each other and are immediately refocussed, diffusion time is reduced, and so is diffusion sensitization of the DWI. Therefore, isotropic weighting appears to come at the price of low diffusion attenuation. A possible solution to this problem may be found in the isotropically weighted sequence proposed simultaneously by Wong and Cox.[41] They searched for gradient sequences in the x, y and z directions that ensured that the off-diagonal elements of the b-matrix elements (i.e. those premultiplying off-diagonal elements of the diffusion tensor) were all zero, while the diagonal elements of the b-matrix elements (i.e. those premultiplying all diagonal elements of the diffusion tensor) were all equal. These constraints, if satisfied, guarantee that the resulting echo magnitude is proportional to trace(**D**). They obtained admissible isotropically weighted sequences using a trial and error search procedure, which intrinsically have higher diffusion weighting than those of Mori and van Zijl, although their complicated pulse shapes make the phase history of the spin system more difficult to interpret.

MEASUREMENTS AND APPLICATIONS OF DIFFUSION ANISOTROPY

We begin by recalling that diffusion anisotropy is a property of certain media in which the translational mobility of the diffusing molecule depends upon the medium's orientation. In biological tissues such as brain white matter, skeletal muscle, soft tissues and cardiac muscle, we can usually ascribe anisotropic diffusion (as measured by MR spectroscopy or imaging) to spatial variations of molecular mobility (heterogeneity) at various length scales ranging from the molecular to the microscopic. Primarily, this phenomenon appears to be due to the presence of ordered macromolecular, membranous, and fibrous compartments and interfaces. Diffusion anisotropy can be characterized within a macroscopic voxel by the effective diffusion tensor, **D**.

Survey of anisotropy measures and indices derived from DWIs

Diffusion anisotropy in tissues has been measured from DWIs using several different scalar indices. Moseley *et al.*[10] characterized diffusion anisotropy in a voxel by the ratio of differences and sums of diffusion-weighted images (DWIs) with diffusion sensitizing gradients applied in two perpendicular directions, e.g. x and y:

$$\frac{\mathrm{DWI}_x-\mathrm{DWI}_y}{\mathrm{DWI}_x+\mathrm{DWI}_y} \tag{21}$$

Douek *et al.*[43] characterized diffusion anisotropy in a voxel by the ratio of two apparent diffusion constants (*ADC*s), again measured with diffusion sensitizing gradients applied in two perpendicular directions, e.g. x and y:

$$\frac{ADC_x}{ADC_y}. \tag{22}$$

In voxels where this ratio was found to be maximal (for a particular tissue type), its value was assumed to be $ADC_\perp/ADC_\parallel$, the ratio of *ADC*s perpendicular to and parallel to the local fiber direction. Finally, van Gelderen *et al.*[35] more recently proposed a scalar anisotropy index that is proportional to the standard deviation of three *ADC*s measured in three mutually perpendicular directions: ADC_x, ADC_y and ADC_z, divided by their mean value, $\langle ADC\rangle$:

$$\frac{\sqrt{(ADC_x-\langle ADC\rangle)^2+(ADC_y-\langle ADC\rangle)^2+((ADC_z-\langle ADC\rangle)^2}}{\langle ADC\rangle}, \tag{23}$$

where $\langle ADC\rangle$ has already been defined in eq. (19).

Besides these indices, several color-coding schemes have been proposed to visualize diffusion anisotropy. Douek *et al.* proposed taking eq. (22) and displaying the ratio as a color image.[43] Subsequently, others have used color-imaging schemes to attempt to elucidate diffusion anisotropy. Nakada *et al.*[44] have proposed using separate R-G-B video channels to display DWI_x, DWI_y and DWI_z, respectively, diffusion-weighted images with sensitizing gradients applied in the three orthogonal directions.

Unfortunately, anisotropy measures based upon DWIs [like eq. (21)] are generally not objective, that is, their contrast does not correspond to a known function of a single

meaningful physical or chemical quantity, but to an unknown function of many such quantities. Second, any anisotropy measure that employs the *ADC* will not be quantitative unless interactions between imaging and diffusion gradients are adequately accounted for as discussed above.[18] However, the feature that all of these anisotropy measures share is that they all inherently depend upon the choice of the laboratory frame of reference, the direction of the applied diffusion gradients, and the orientation of the macromolecular, cellular and/or fibrous structures within the tissue in each voxel. Like the *ADC*, they are not invariant. As a result, their values will change, for example, when the sample is rotated within the magnet. These measures inherently introduce a directional artifact into the measurement of anisotropy. Pierpaoli *et al.*[25] recently demonstrated this point convincingly, showing that when one uses eq. (23), the anisotropic white matter in the ventral internal capsule of the brain appears isotropic like gray matter. Moreover, this error, predicted by theoretical considerations alone, depends upon the relative orientation of the white matter structure and the x, y and z laboratory coordinate frame of reference.

Anisotropy indices that use the *ADC*, such as eq. (23), are estimated without accounting for the effect of imaging gradients on the measured NMR signal. The error made by this omission depends upon the particular imaging sequence used. To estimate its severity we see from eq. (2) that

$$-\sum_{i=1}^{3}\sum_{j=1}^{3}\Delta b_{ij}D_{ij}=\sum_{i=1}^{3}\sum_{j=1}^{3}b_{ij}\Delta D_{ij}, \tag{24}$$

from which one can show that the fractional error in calculating a b-matrix element approximately equals the fractional error in its corresponding diffusion tensor element that we estimate. In the diffusion weighted two-dimensional-FT spin echo sequences we have used, we would routinely calculate errors of 10–15% in the estimates of the diagonal elements of **D** if we failed to account for imaging gradients.[18] This error is further exacerbated by ignoring the off-diagonal elements of **D** when attempting to estimate the diagonal elements of **D** in anisotropic media.[20]

An alternative approach to characterizing diffusion anisotropy has been to derive scalar invariant quantities from the diffusion tensor that represent some feature of anisotropic diffusion while being invariant quantities.[45] This is because an anisotropy index should be physically meaningful, as well as being intrinsic to the tissue. As such, it should be independent of the sample's placement or orientation with respect to the (laboratory) x-y-z reference frame. Several quantities described below satisfy these criteria.

One proposed set of anisotropy indices, the ratios of the principal diffusivities,[15] measures features of the shape (degree of prolateness) of the diffusion ellipsoid, but is independent of its size and orientation. These dimensionless ratios measure the relative effective diffusivities in the three principal directions. For example, if we number the principal diffusivities in decreasing order, the dimensionless anisotropy ratio, λ_2/λ_3, then measures the degree of cylindrical symmetry (with $\lambda_2/\lambda_3=1$ indicating perfect cylindrical symmetry). Alternatively, one could calculate the eccentricity, ε, of the great ellipse that lies in the plane normal to the fiber-tract axis and divides the diffusion ellipsoid into two equal pieces:

$$\varepsilon=\frac{\sqrt{\lambda_2-\lambda_3}}{\sqrt{\lambda_2}}. \tag{25}$$

To measure the relative magnitude of the diffusivities along the fiber-tract direction and the two transverse directions, we can calculate λ_1/λ_2 and λ_1/λ_3, or, as above, measure the eccentricities of the two remaining great ellipses obtained from the diffusion ellipsoid that also contain its major axis (i.e. the axis along the fiber-tract direction).*

Pierpaoli *et al.*[25] recently suggested a scalar invariant, dimensionless anisotropy index that includes all three principal diffusivities:

$$\text{Volume ratio}=\frac{\lambda_1\lambda_2\lambda_3}{\left(\frac{\lambda_1+\lambda_2+\lambda_3}{3}\right)^3}=27\frac{\text{Determinant}(\mathbf{D})}{\text{Trace}(\mathbf{D})^3} \tag{26}$$

Rotational invariance is assured because this measure depends solely on the ratio of two scalar invariants computed from the diffusion tensor, its determinant and its trace. The volume ratio is aptly named because it represents the square of the volume of the diffusion ellipsoid divided by the square of the volume of a diffusion sphere whose radius is the square root of mean diffusivity, $\langle D\rangle$, defined above in eq. (16). Images of the volume ratio for living monkey brain are qualitatively similar to those of the anisotropy ratio image, λ_1/λ_3,[25] in that the intensity of voxels containing gray matter and CSF-filled ventricles is virtually the same, while the intensity in voxels containing white matter is significantly different. However, the volume ratio is generally less noisy than the ratio of eigenvalues.[25]

Basser and Pierpaoli[45] more recently proposed another measure of diffusion anisotropy that was actually derived from the diffusion tensor. It uses the requirements that (a) the anisotropy measure is a scalar invariant quantity and (b) it measures the magnitude of the anisotropic part of the diffusion tensor, D. One proposed measure that possesses these properties is given by $D:D$, where

$$D:D=(D_{xx}-\langle D\rangle)^2+(D_{yy}-\langle D\rangle)^2+(D_{zz}-\langle D\rangle)^2 +2D_{xy}^2+2D_{xz}^2+2D_{yz}^2, \tag{27}$$

and, again, using the definition of $\langle D\rangle$ given in eq. (16). The first three terms on the right-hand side of eq. (27) are the sum of the square deviations between the diagonal elements of D and their mean value, $\langle D\rangle$; the remaining three terms are the sum of the squares of the *off*-diagonal elements of D. Thus $D:D$ is the scalar measure of the degree to which the diffusion tensor deviates from isotropy (in a mean-squared sense). In the principal or fiber-tract frame, all off-diagonal elements of D vanish (i.e. $D_{xy}=D_{xz}=D_{yz}=0$) and its diagonal elements, D_{xx}, D_{yy} and D_{zz}, are replaced by the principal diffusivities, λ_1, λ_2 and λ_3. Then,

$$D:D=(\lambda_1-\langle D\rangle)^2+(\lambda_2-\langle D\rangle)^2+(\lambda_3-\langle D\rangle)^2 \tag{28}$$

where again $\langle D\rangle$ is defined as above in eq. (16). This quantity clearly is a scalar invariant because it is a function solely of the eigenvalues of D, and is independent of their assignment or ordering scheme. (Any permutation of the indices 1, 2 and 3 will produce the same result). Equation (28) also provides a more satisfying interpretation of $D:D$. It is the sum of the squares of the deviations between the

* While the ratios of the eigenvalues of **D** represent the ratios of its principal diffusivities, it may be preferable to measure the ratios of the mean-squared diffusion distances. This can be done simply by taking the square roots of the ratios presented above, i.e. $\sqrt{\lambda_i/\lambda_j}$.

principal diffusivities of D and their mean value—the mean diffusivity, $\langle D\rangle$. Now, by taking the "magnitude" of the anisotropic part of D and dividing it by the "magnitude" of the isotropic part of D, we obtain a dimensionless measure of the relative anisotropy, RA:[45]

$$RA=\frac{1}{\sqrt{3}}\frac{\sqrt{D:D}}{\langle D\rangle}$$

$$=\frac{1}{\sqrt{3}}\frac{\sqrt{(\lambda_1-\langle D\rangle)^2+(\lambda_2-\langle D\rangle)^2+(\lambda_3-\langle D\rangle)^2}}{\langle D\rangle}, \quad (29)$$

which is quantitative (i.e. physically meaningful and invariant). For an isotropic medium $RA=0$. It is instructive to compare eq. (29), which is invariant, with eq. (23), which is not.

Alternatively, if we are interested in measuring the fractional anisotropy, FA, (i.e. the fraction of the total "magnitude" of the diffusion tensor that we can ascribe to anisotropic diffusion) we have proposed the following expression:[45]

$$FA=\frac{3}{2}\frac{\sqrt{D:D}}{\sqrt{\mathbf{D}:\mathbf{D}}}. \quad (30)$$

For an isotropic medium, $FA=0$; for a cylindrically symmetric anisotropic medium (with $\lambda_1 \gg \lambda_2=\lambda_3$), then $FA=1$.

If one were now interested in developing a color coding scheme to visualize diffusion anisotropy, it would be recommended to make the assignment of the colors invariant, or independent of the laboratory coordinate frame, etc. This could be done, for example, by following the clever suggestion of Larry Latour's at the recent 1995 Workshop on Diffusion (London). He proposed using separate R-G-B video channels to represent the three principal diffusivities, λ_1, λ_2 and λ_3. Unlike other proposed color-based measures of anisotropy (e.g. Ref. 44), this one would not introduce an orientational artifact (e.g. change of color when the tissue is rotated). For this new color scheme to work, one should sort the eigenvalues consistently in each voxel, for example, in decreasing order. However, one should be cognizant that sorting of the eigenvalues introduces a significant statistical bias, particularly for low S/N,[46] which could affect the color in each voxel and its distribution.

In summary, characterizing diffusion anisotropy is tantamount to characterizing the shape of a diffusion ellipsoid, independent of its orientation and size. It is then easy to see that knowing only the diagonal elements of the diffusion tensor is not adequate to characterize diffusion anisotropy. Knowing the eigenvalues of the diffusion tensor is sufficient, but since in most MRI applications we typically do not know them *a priori* we generally must determine them using both the diagonal and off-diagonal elements of **D**.

CYLINDRICAL SYMMETRY AND THE DIFFUSION TENSOR

Several studies have been published recently assuming that diffusion is cylindrically symmetric about the fiber-tract axis in nerve white matter[47,48] and in skeletal muscle fibers[49,50] (the former having used this assumption to simplify the measurement of fiber orientation[43,48]). This is tantamount to presuming that the diffusion ellipsoid is symmetric about its (longest) major axis, i.e. it is a surface of revolution about the fiber-tract axis. This assumption is seductive because it allows us to reduce the number of independent elements of the diffusion tensor from six to four. While it is good practice to use whatever *a priori* information is available to improve the estimate of **D**, it is recommended that each assumption first be tested experimentally. If this is not possible, then we suggest testing the assumption of cylindrical symmetry *a posteriori* within each voxel. This could be done by testing the null hypothesis that the two smallest eigenvalues (or principal diffusivities) of the diffusion tensor are equal. Then, one can assess whether the hypothesis of cylindrical symmetry must be rejected or accepted based upon the measured data. Hypothesis testing in the context of diffusion tensor imaging, however, has a precedent: it was used to test whether a diffusion tensor is isotropic or anisotropic.[20]

There are a number of practical reasons discussed below why diffusion would not be (or at least appear not to be) cylindrically symmetric in tissues. Firstly, partial volume artifacts will affect the apparent symmetry of the measured diffusion tensor.[46] In the brain, for example, some voxels may contain a mixture of gray matter, CSF and white matter, each with its own diffusion tensor. Moreover, in white matter, there may be more than a single fiber tract direction within a voxel, as fibers may be crossing each other or radiating in different directions.[46,51] The estimated tensor will be a weighted average of the diffusion tensors of these various tissue compartments. Secondly, noise in the DWIs would tend to make cylindrically symmetric media appear to be cylindrically asymmetric.[46,51] Specifically, the two smallest estimated eigenvalues, λ_2 and λ_3, would be expected to be different from one another in many voxels owing to measurement noise, an effect that is exacerbated as S/N is reduced. Thirdly, anatomically there may be barriers to diffusion (ranging from the macromolecular to cellular length scales) as well as local defects and dislocations that will make diffusion cylindrically asymmetric. This issue is under considerable debate in the cardiovascular field.[52] A recent paper by Garrido *et al.* also suggested that the assumption of cylindrical symmetry does not apply in the rat heart and so does the recent work of Wedeen *et al.*[53] Moreover, the loss of cylindrical symmetry in some voxels may have some diagnostic or clinical value.

To resolve this problem, we could test the hypotheses of cylindrical symmetry and then that of spherical symmetry (i.e. isotropy) sequentially, voxel by voxel. For the given background noise level, if the hypothesis of cylindrical symmetry is rejected, the diffusion tensor representation should be retained. Otherwise, a reduced set of parameters (e.g. Hsu's and Mori's[47]) could be used to represent the diffusion tensor. Then, if the test of the hypothesis of isotropy is supported, the diffusion coefficient is the only transport coefficient required to describe diffusion in that voxel. In this way, the diffusion process in each voxel is represented most economically, and the parameters of the model will be estimated with the lowest variance.

RESTRICTED DIFFUSION AND THE DIFFUSION TENSOR

Restricted diffusion refers to the case in which a diffusing species encounters reflecting boundaries that sequester it

within a particular compartment. This term applies, for example, to the diffusion of intracellular markers. In a restricted geometry, diffusion on a macroscopic scale no longer appears to be Gaussian; specifically the effective probability density function within a voxel can no longer be fit adequately using Eq. (8). Geometrically, in restricted diffusion the surface of constant mean-squared displacement is no longer ellipsoidal in shape. Equivalently, the Einstein equation relating the mean-squared molecular displacement and the diffusion time no longer applies along the directions perpendicular to the reflecting boundaries, and the physical meaning of the diffusion coefficient as well as the diffusion tensor elements associated with these directions becomes moot. Nonetheless, some groups have attempted to use the diffusion tensor formalism to describe diffusion of a molecule in restricted compartments. This is the case in a recent study of phosphocreatine (an intracellular marker) in rabbit leg muscle.[50] In such cases, we recommend measuring the displacement distribution of the diffusing species directly using q-space methods.[54, 55]

Fiber orientation and architectural imaging

The ability to measure the diffusion tensor has also created the opportunity to measure fiber-tract direction fields and other architectural features of tissues. The first measurement of the fiber-tract direction using diffusion tensor methods was performed spectroscopically on skeletal muscle.[31] The anatomical fiber tract directions were seen to be coincident with the principal direction or axis of the diffusion ellipsoid associated with the largest principal diffusivity.[15, 31, 56] Shortly thereafter, diffusion tensor images were obtained of skeletal muscle *in vitro*,[15] white matter *in vitro*[15, 57] and *in vivo*[58, 59], and more recently in cardiac tissue.[7, 52, 53] Quantitative, rapid, high-quality, high-resolution, clinical DTI was realized recently, providing images suitable for radiological evaluation.[38] Recently Reese *et al.* published a technical *tour de force* demonstrating how diffusion tensor imaging methods can be extended to elucidate tissue architecture in a beating human heart.[60]

Diffusion tensor MRI provides unique tools with which to probe tissue structure at different levels of hierarchical organization. While experimental diffusion times are consistent with measurements of molecular displacements on the order of microns, these molecular motions are then averaged within voxels, which are then assembled into multi-slice or three-dimensional images of tissues or organs. This single imaging method then permits us to elucidate complex structural features from the macromolecular to the macroscopic length scales. Recently, several new invariant parameters have been proposed that help assess both intra- and intervoxel macrostructural features.[45]

CONCLUDING REMARKS

One recurring theme in this review is that the effective diffusion and measurement ellipsoids can help us understand how to characterize and measure diffusion in isotropic and anisotropic media simply by examining their features, such as their size, shape, orientation and pattern. Another important theme is that if one is interested in using a scalar quantity to characterize some intrinsic feature of an anisotropic medium, such as the degree of diffusion anisotropy or fiber organization; that parameter should be invariant to translation and rotation of the laboratory coordinate system. If, in addition, these parameters are physically meaningful, they will possess characteristics of a quantitative physiological or histological stain.

We have also seen that some confusion arises from using inappropriate models of diffusion to interpret diffusion weighted images. In an isotropic medium, we can use an isotropic model of diffusion [as in eq. (3)]. In an anisotropic medium, it is appropriate to use an anisotropic model of diffusion—diffusion tensor imaging [as in eq. (2)]. In restricted media, it is appropriate to use q-space imaging methods.

REFERENCES

1. Taylor, D. G. and Bushell, M. C. The spatial mapping of translational diffusion coefficients by the NMR imaging technique. *Phys. Med. Biol.* **30**, 345–349 (1985).
2. Merboldt, K. D., Hanicke, W. and Frahm, J. Self-diffusion NMR imaging using stimulated echoes. *J. Magn. Reson.* **64**, 479–486 (1985).
3. Le Bihan, D. and Breton, E. Imagerie de diffusion *in vivo* par resonance magnetique nucleaire. *Cr. Acad. Sci.* (Paris) **301**, 1109–1112 (1985).
4. Le Bihan, D. Diffusion NMR imaging. *Magn. Reson. Q.* **7**, 1–30 (1991).
5. Le Bihan, D. *Diffusion and Perfusion Magnetic Resonance Imaging.* Raven, New York (1995).
6. Turner, R., Le Bihan, D., Maier, J., Vavrek, R., Hedges, L. K. and Pekar, J. Echo-planar imaging of intravoxel incoherent motion. *Radiology* **177**, 407–414 (1990).
7. Garrido, L., Wedeen, V. J., Kwong, K. K., Spencer, U. M. and Kantor, H. L. Anisotropy of water diffusion in the myocardium of the rat. *Circ. Res.* **74**, 789–793 (1994).
8. Cleveland, G. G., Chang, D. C., Hazlewood, C. F. and Rorschach, H. E. Nuclear magnetic resonance measurement of skeletal muscle: anisotropy of the diffusion coefficient of the intracellular water. *Biophys. J.* **16**, 1043–53 (1976).
9. Henkelman, R. M. Does IVIM measure classical perfusion? *Magn. Reson. Med.* **16**, 470–475 (1990).
10. Moseley, M. E., Cohen, Y., Kucharczyk, J., Mintorovitch, J., Asgari, H. S., Wendland, M. F., Tsuruda, J. and Norman, D. Diffusion-weighted MR imaging of anisotropic water diffusion in cat central nervous system. *Radiology* **176**, 439–445 (1990).
11. Tanner, J. E. Self diffusion of water in frog muscle. *Biophys. J.* **28**, 107–116 (1979).
12. Doran, M., Hajnal, J. V., Van Bruggen, N., King, M. D., Young, I. R. and Bydder, G. M. Normal and abnormal white matter tracts shown by MR imaging using directional diffusion weighted sequences. *J. Comput. Assist. Tomogr.* **14**, 865–873 (1990).
13. Chenevert, T. L., Brunberg, J. A. and Pipe, J. G. Anisotropic diffusion in human white matter: demonstration with MR techniques *in vivo*. *Radiology* **177**, 401–405 (1990).
14. Basser, P. J. Elucidating tissue structure and physiology via diffusion tensor MRI. *J. Magn. Reson.* (1996).
15. Basser, P. J., Mattiello, J. and Le Bihan, D. MR diffusion tensor spectroscopy and imaging. *Biophys. J.* **66**, 259–267 (1994).
16. Crank, J. *The Mathematics of Diffusion*, 2nd edn. Oxford University Press, Oxford (1975).
17. Le Bihan, D. Molecular diffusion nuclear magnetic resonance imaging. *Magn. Reson. Q.* **7**, 1–30 (1991).
18. Mattiello, J., Basser, P. J. and Le Bihan, D. Analytical

expression for the *b*-matrix in NMR diffusion imaging and spectroscopy. *J. Magn. Reson. A* **108**, 131–141 (1994).
19. Basser, P. J., Mattiello, J. and Le Bihan, D. Diagonal and off-diagonal components of the self-diffusion tensor: their relation to and estimation from the NMR spin-echo signal. *11th Annual Meeting of the SMRM.* Abstr., p. 1222 (1992).
20. Basser, P. J., Mattiello, J. and Le Bihan, D. Estimation of the effective self-diffusion tensor from the NMR spin echo. *J. Magn. Reson. B* **103**, 247–254 (1994).
21. Mattiello, J., Basser, P. J. and Le Bihan, D. Analytic expressions for the *b*-matrix in diffusion tensor echo-planar imaging. *Magn. Reson. Med.* (1995) (submitted).
22. Einstein, A. *Investigations on the Theory of the Brownian Movement.* Dover Publications, New York (1926).
23. Rao, C. R. *Linear Statistical Inference and its Applications.* Wiley, New York (1965).
24. Carr, H. Y. and Purcell, E. M. Effects of diffusion on free precession in nuclear magnetic resonance experiments. *Phys. Rev.* **94**, 630–638 (1954).
25. Pierpaoli, C., Mattiello, J., Le Bihan, D., DiChiro, G. and Basser, P. J. Diffusion tensor imaging of brain white matter anisotropy. *13th Annual Meeting of the SMRM.* Abstr., p. 1038 (1994).
26. Moseley, M. E., Kucharczyk, J., Mintorovitch, J., Cohen, Y., Kurhanewicz, J., Derugin, N., Asgari, H. and Norman, D. Diffusion-weighted MR imaging of acute stroke: correlation with T_2-weighted and magnetic susceptibility-enhanced MR imaging in cats. *Am. J. Neuroradiol.* **11**, 423–442 (1990).
27. Moseley, M. E., Cohen, Y., Mintorovitch, J., Chileuitt, L., Shimizu, H., Kucharczyk, J., Wendland, M. F. and Weinstein, P. R. Early detection of regional cerebral ischemia in cats: comparison of diffusion- and T_2-weighted MRI and spectroscopy. *Magn. Reson. Med.* **14**, 330–346 (1990).
28. Mintorovitch, J., Moseley, M. E., Chileuitt, L., Shimizu, H., Cohen, Y. and Weinstein, P. R. Comparison of diffusion- and T_2-weighted MRI for the early detection of cerebral ischemia and reperfusion in rats. *Magn. Reson. Med.* **18**, 39–50 (1991).
29. Chien, D., Kwong, K. K., Gress, D. R., Buonanno, F. S., Buxton, R. B. and Rosen, B. R . MR diffusion imaging of cerebral infarction in humans. *AJNR Am. J. Neuroradiol.* **13**, 1097–1102; discussion 1103–1105 (1992).
30. Warach, S., Chien, D., Li, W., Ronthal, M. and Edelman, R. R. Fast magnetic resonance diffusion-weighted imaging of acute human stroke. *Neurology* **42**, 1717–1723 (1992) (published erratum appears in *Neurology* **42**, 2192 (1992).
31. Basser, P. J. and Le Bihan, D. Fiber orientation mapping in an anisotropic medium with NMR diffusion spectroscopy. *11th Annual Meeting of the SMRM.* Abstr., p. 1221 (1992).
32. Basser, P. J., Mattiello, J., Turner, R. and Le Bihan, D. Diffusion tensor echo-planar imaging of human brain, *12th Annual Meeting of the SMRM.* Abstr., p. 1404 (1993).
33. Basser, P. J. Fiber orientation mapping in anisotropic media with NMR. *BMES '92 Annual Conf.* (1992).
34. Kärger, J., Pfeifer, H. and Heink, W. Principles and applications of self-diffusion measurements by nuclear magnetic resonance, edited by J. Waugh. In *Advances in Magnetic Resonance*, vol. 12, pp. 1–89. Academic Press, London (1988).
35. van Gelderen, P., Vleeschouwer, M. H. M. d., DesPres, D., Pekar, J., van Zijl, P. C. M. and Moonen, C. T. W. Water diffusion and acute stroke. *Magn. Reson. Med.* **31**, 154–163 (1994).
36. Stejskal, E. O. and Tanner, J. E. Spin diffusion measurements: spin echoes in the presence of time-dependent field gradient. *J. Chem. Phys.* **42**, 288–292 (1965).
37. Jezzard, P. and Pierpaoli, C. Diffusion mapping using interleaved spin echo and STEAM EPI with navigator echo correction. *SMR/ESMRMB.* Abstr., p. 903 (1995).
38. Pierpaoli, C., Jezzard, P. and Basser, P. High-resolution diffusion tensor imaging of the human brain. *SMR/ESMRMB.* Abstr., p. 899 (1995).
39. Edelman, R. R., Gaa, J., Wedeen, V. J., Loh, E., Hare, J. M., Prasad, P. and Li, W. *In vivo* measurement of water diffusion in the human heart. *Magn. Reson. Med.* **32**, 423–428 (1994).
40. Mori, S. and van Zijl, P. C. Diffusion weighting by the trace of the diffusion tensor within a single scan. *Magn. Reson. Med.* **33**, 41–52 (1995).
41. Wong, E. C. and Cox, R. W. Single-shot imaging with isotropic diffusion weighting. *2nd Annual Meeting of the SMR.* Abstr., p. 136 (1994).
42. Wong, E. C., Cox, R. W. and Song, A. W. Optimized isotropic diffusion weighting. *Magn. Reson. Med.* **34**, 139–143 (1995).
43. Douek, P., Turner, R., Pekar, J., Patronas, N. and Le Bihan, D. MR color mapping of myelin fiber orientation. *J. Comput. Assist. Tomogr.* **15**, 923–9 (1991).
44. Nakada, T., Matsuzawa, H. and Kwee, I. L. Magnetic resonance axonography of the rat spinal cord. *Neuroreport* **5**, 2053–2056 (1994).
45. Basser, P. and Pierpaoli, C. Elucidating tissue structure by diffusion tensor MRI. *SMR/ESMRMB.* Abstr., p. 900 (1995).
46. Pierpaoli, C. and Basser, P. J. Toward a quantitative measure of diffusion anisotropy. *Magn. Reson. Med.* (1995) (submitted).
47. Hsu, E. W. and Mori, S. Analytical expressions for the NMR apparent diffusion-coefficients in an anisotropic system and a simplified method for determining fiber orientation. *Magn. Reson. Med.* **32**, 194–200 (1995).
48. Coremans, J., Luypaert, R., Verhelle, F., Stadnik, T. and Osteaux, M. A method for myelin fiber orientation mapping using diffusion-weighted MR images. *Magn. Reson. Imag.* **12**, 443–454 (1994).
49. Yang, Y., Shimony, J. S., Xu, S., Gulani, V., Dawson, M. J. and Lauterbur, P. C. A sequence for measurement of anisotropic diffusion by projection reconstructon imaging and its application to skeletal and smooth muscle. *2nd Annual Meeting of the SMR.* Abstr., P. 1036 (1994).
50. van Gelderen, P., DesPres, D., van Zijl, P. C. and Moonen, C. T. Evaluation of restricted diffusion in cylinders. Phosphocreatine in rabbit leg muscle. *J. Magn. Reson. B* **103**, 255–260 (1994).
51. Pierpaoli, C. and Basser, P. J. New Invariant 'Lattice' Index Achieves Significant Noise Reduction in Measuring Diffusion Anisotropy *Proceedings of the ISMRM.* Abstr., 1326 (1996).
52. Le Grice, I. J. and Al, E. Laminar structure of the heart: ventricular myocyte arrangement and connective tissue architecture in the dog. *Am. J. Phys.* **269**, H571-H582 (1995).
53. Wedeen, V. J., Reese, T. G., Smith, R. N. and Rosen, B. R. Mapping myocardial architecture with diffusion anisotropy MRI. *Proc. SMR and ESMRMB.* Abstr., p. 357 (1995).
54. Callaghan, P. T., Eccles, C. D. and Xia, Y. NMR microscopy of dynamic displacements: *k*-space and *q*-space imaging. *J. Phys. E. Sci. Instrum.* **21**, 820–822 (1988).
55. King, M. D., Houseman, J., Roussel, S. A., van Bruggen, N., Williams, S. R. and Gadian, D. G. *q*-Space imaging of the brain. *Magn. Reson. Med.* **32**, 707–713 (1994).
56. Basser, P. J., LeBihan, D. and Mattiello, J. Measuring tissue fiber direction using diffusion NMR. *37th Annual Meeting of the Biophysical Society.* Abstr., p. 131 (1993).
57. Basser, P. J., Mattiello, J. and LeBihan, D. MR imaging of fiber-tract direction and diffusion in anisotropic tissues. *12th Annual Meeting of the SMRM.* Abstr., p. 1403 (1993).
58. Basser, P. J., Mattiello, J., Turner, R. and Le Bihan, D. Diffusion tensor echo-planar imaging (DTEPI) of human brain. *SMRM Workshop: Functional MRI of the Brain.* Abstr., p. 224 (1993).
59. Davis, T. L., Wedeen, V. J., Weisskoff, R. M. and Rosen, B. R. White matter tract visualization by echo-planar MRI. *SMRM 12th Annual Meeting.* Abstr., p. 289 (1993).
60. Reese, T. G., Weissdoff, R. M., Smith, R. N., Rosen, B. R., Dinsmore, R. E. and Wedeen, V. J. Imaging myocardial fiber architecture *in vivo* with magnetic resonance. *Magn. Reson. Med.* **34**, 786–791 (1995).